

The effects of alternating current (AC) electrification on the tribological performance of gear materials with internal combustion engine (ICE) and electric vehicle (EV) transmission lubricants

Tribology - Materials, Surfaces & Interfaces

2024, Vol. 18(4) 270–283

© The Author(s) 2024



Article reuse guidelines:

sagepub.com/journals-permissions

DOI: 10.1177/17515831241301166

journals.sagepub.com/home/trb



Thawhid Khan¹ , Joshua L Armitage² and Michael G Bryant³

Abstract

Electric Vehicles (EVs) present a vastly different set of tribological challenges to internal combustion engine (ICE) vehicles. Not only does the high torque production and high rotor speeds experienced in EV motors extenuate existing tribological challenges in the automotive sector; the inherent electrified nature of EV drivetrains is a key challenge. Many forms of stray electric current are prevalent within such systems, which cause the deterioration of key mechanical components through several electrochemical and electromechanical wear mechanisms. In this study, a novel electromechanical apparatus has been implemented to investigate the effects of alternating current (AC) discharge across ball-on-disc unidirectional sliding contacts, lubricated by commercially available transmission fluids. Three lubricants were compared at 80°C under both unelectrified and AC conditions. The three lubricants were used: a group IV poly- α -olefin (PAO 4) synthetic base oil and two commercially available transmission fluids – currently implemented within ICE vehicles and EVs, respectively. The key findings of this study highlight a reduction in friction under electrified conditions, combined with expedited material wear and tribochemical surface modification. The friction behaviour of the ICE transmission lubricant deteriorated over time due to electrification causing fluid property degradation.

Keywords

electrified sliding, e-fluids, electric vehicles, transmission fluid, tribo-oxidation

Received: 10 October 2024; accepted: 4 November 2024

Introduction

Owing to the increasing limitation of global petroleum resources, in combination with the ever-growing urgency for a reduction in global CO₂ emissions,¹ the push for research into alternative power sources for commercial and passenger vehicles has never been stronger. This has led to the development of various forms of alternative powertrain solutions; from the use of alternative ICE fuels such as hydrogen (H₂)² and ammonia (NH₃),³ to the use of fuel cells (FCEVs), hybrid ICE generators (HEVs), and batteries (BEVs) for powering electric motors (EMs).⁴

Because of this wide variety of available powertrain configurations, EVs utilise many different and uniquely challenging driveline architectures compared to traditional ICE systems. These systems generally tend to operate in harsher conditions – involving rotational speeds of up to 25,000 RPM and torques of up to several kNm – even at low speeds.^{5,6} EMs also tend to overheat and reduce efficiency at temperatures above 95°C, which implies that

thermal management is a critical factor to consider in the design of EV powertrains and their lubricants.⁷ The varying driveline architectures for EVs also differ from those of ICEVs in several distinct ways. The role of tribological contacts within EV drivetrains leans more towards the transference of torque, rather than the load bearing characteristics of contacts within ICE drivetrains.⁵

Automatic Transmission Fluids (ATFs) were initially implemented within early iterations of EV drivetrains as a

¹Department of Mechanical Engineering, University of Sheffield, Sheffield, UK

²Institute of Functional Surfaces, University of Leeds, School of Mechanical Engineering, Leeds, Yorkshire, UK

³University of Birmingham, School of Mechanical Engineering, Edgbaston, West Midlands, UK

Corresponding author:

Thawhid Khan, Department of Mechanical Engineering, University of Sheffield, Mappin Street, Sheffield, S1 3JD, UK.

Email: thawhidkhan@yahoo.co.uk

way of addressing their tribological challenges with existing products.⁸ ATFs generally demonstrate favourable electrical resistances and dielectric breakdown strengths, in addition to previously demonstrating some resistance to copper corrosion, aeration, and oxidation within their existing applications.⁹ However, there are rarely friction clutches within EV transmissions, which implies that some additives within common ATFs may not be necessary within the formulation of EV transmission fluids. The thermal properties of ATFs are also not optimised for EV systems. Some EV transmissions may operate at similar temperatures to traditional transmission systems ($\sim 80^\circ\text{C}$), EV transmissions that are located in proximity to, or incorporate their respective EMs can be subjected to much greater sources of heat and must therefore be able to transfer it away to maintain this optimum operating temperature.⁷ Owing to these differences in operating conditions, dedicated fluids for EVs – termed ‘e-fluids’¹⁰ have now been developed to act as both a lubricant and coolant for such systems.

In addition to these changes in tribological and thermal system characteristics, the inherent electrified nature of EV drivetrains also poses its own series of unique challenges. Inverters operate as the beating heart of EV transmissions, converting the high-voltage (300–1000 V) direct current (DC) output to a sinusoidal three-phase alternating current (AC) output using pulse-wave modulation (PWM).¹¹ Inverters also work as variable frequency drives (VFDs) to adjust the frequency ($f = 10\text{--}20\text{ kHz}$) and root-mean-square current amplitude ($I_{RMS} = 230\text{--}600\text{ A}$) of this AC output to match the needs of the EM. A direct result of these high-frequency high-current inverter outputs is the propagation of adverse shaft currents and electromagnetic fields throughout an EV drivetrain during EM operation, often referred to as ‘stray’ currents.¹² The intensity and duration of these stray currents depend greatly on the drivetrain architecture and EMs being utilised.¹³ Additionally, magnetic flux asymmetries – caused by the inconsistencies in shaft designs – can generate low frequency voltage waves.¹⁴

These stray currents and fields can travel through mechanical components such as synchronisers, bearings, and gears – affecting their tribological performance.^{15–19} Full-film lubrication often allows for voltage build-up across the dielectric lubricant layer.²⁰ When the electric field applied to such a contact exceeds the dielectric strength of the lubricant, an electrical arc discharge will occur across it.²¹ The energy densities of these arcs at contacting interfaces are often high enough – owing to the concentrated sizes of asperity-asperity contacts – to cause the localised melting and subsequent removal of asperities, leaving μm -sized pits wherever these discharges occur.¹² The high switching rates of EV inverters also implies that these discharge events occur at similarly high frequencies. One typically observed symptom of EDM within EVs is referred to as ‘electrical frosting’, which manifests as the formation of a grey band within raceways & contacts as EDM pits become evenly distributed across them. Electrical frosting is shown to eventually lead to fluting

and furrowing, which ultimately leads to fluid film collapse and more critical component failures.¹² This unintentional form of EDM additionally leads to changes in chemical composition – both of the participating surfaces as well as the conducting lubricant – which in-turn leads to degradation and fatigue within the contact. However typical EDM wear from high-energy discharges might not appear under the lower current conditions used in this study.

Several previous studies have investigated the impact of direct current (DC) electrification on friction and wear behaviour of lubricated metallic contacts through tribo-electrochemical analyses.²² Key hypotheses have focused on the effect of electrical currents on the adsorption and/or desorption of additives to surfaces during sliding. The impact of electrification on redox reactions due to the presence of oxygen and lubricant additives has also been a key focus.^{22–25}

Existing studies have also investigated the effects of 50 Hz AC electrification on various forms of rolling bearing contacts.^{26,27} Whilst both approaches provide valuable insights into the effects of DC electrification on additive lubrication and AC electrification on rolling contacts, they ultimately are not designed to address the unique combination of tribological factors and high-frequency AC electrification observed within EV systems. This research integrates elements from existing methods to explore how alternating current (AC) potentials impact friction, wear, and the formation of tribofilms in commercial internal combustion engine (ICE) and electric vehicle (EV) transmission fluids. The study focuses on contacts that closely mimic the helical gear interfaces typically found in EV powertrains.

Methodology

In order to sufficiently evaluate the effects of AC electrification within lubricated sliding contacts at temperature, a novel tribometry apparatus was implemented in combination with a range of ex-situ pre- and post-test analyses.

Tribological testing

A bespoke ball-on-disc tribometer (Bruker UMT TriboLab, USA) was developed to apply various forms of electric potential to a lubricated unidirectional sliding contact at an elevated temperature, as shown in Figure 1.

The ball-on-disc arrangement involves loading an upper spherical sample with a pre-defined normal force (F_z) against the flat face of a lower rotating disc sample. The upper ball sample is secured to a two-dimensional strain-gauge load-cell (capacity of $\pm 50\text{ N}$ with a resolution of 2.5 mN), with its position relative to the lower sample being precisely controlled via two orthogonal screw-driven linear actuators. The upper sample was contacted with the lower disc sample a distance (r_θ) of 16 mm from its centre of rotation, allowing for a sliding speed (v) of 0.1 ms^{-1} at a rotation frequency (f) of 1 Hz. The 2D load-cell was oriented tangentially to the direction of rotation, allowing for the measurement torque (τ) through lateral force measurement ($F_x = \tau / r_\theta$) in addition to measuring F_z . Previous studies

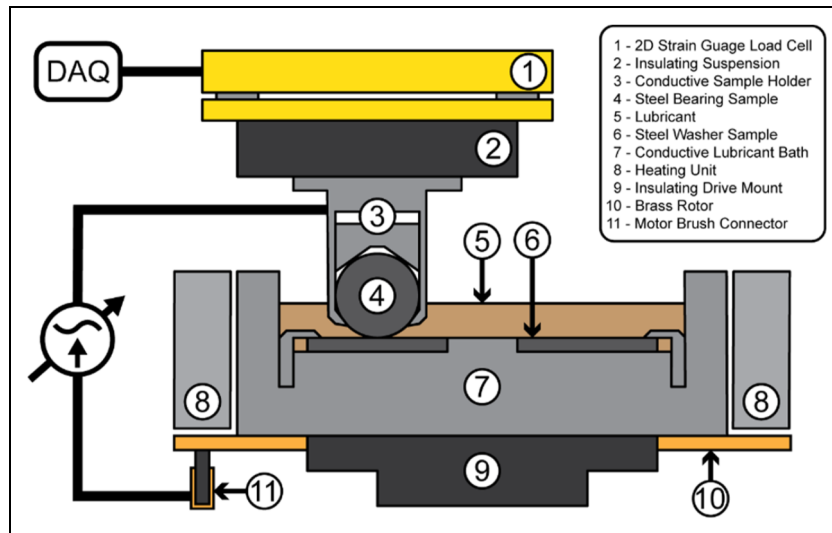


Figure 1. Schematic depiction of the ball-on-disc set-up.

Table 1. Summary of ball-on-disc test conditions.

Parameter	Value
RMS current (I_{RMS} , A)	0, 2
Normal force (F_z , N)	15
Hertzian contact pressure (P_{max} , MPa)	985
Sliding speed (v , ms^{-1})	0.1
Test duration (mins)	120
Lubricant temperature (T , °C)	80
Oil quantity per test (mL)	25
Test repeats	3

have shown that contact pressures within transmission systems range from 900–1080 MPa.²⁸ A normal force of 15 N was applied in this study to achieve a maximum contact pressure (P_{max}) of 985 MPa which suitably fits within this range. A proportional-integral-derivative (PID) controller allowed for the vertical position of the upper sample to be adjusted in order to maintain a consistent F_z as the lower sample is rotated. The friction coefficient (μ) as a function of test duration (t) for the sliding contact was determined by Equation (1).

$$\mu(t) = \frac{F_x(t)}{F_z(t)} \quad (1)$$

The lower disc samples were positioned in a brass lubricant bath, able to hold 25 mL of lubricant and fully immersing the sliding contact throughout the test duration. The lubricant bath is contained within a heating unit, capable of heating the arrangement to 80°C without physically contacting any component. A thermocouple was also immersed into the lubricant to monitor and maintain a consistent lubricant temperature. A schematic of the tribometry arrangement is given in Figure 1, with a summary of in-situ test parameters given in Table 1.

Materials & lubricants

The ball and disc samples were both composed of 52,100 bearing steel. The ball samples were Ø12 mm grade 100

bearings, hardened to 60–67 HRC. The disc samples were washers – hardened to 196.7 HV₁, having a 42 mm outer diameter, 25 mm inner diameter, and 1 mm thickness. The centre-plane arithmetic mean surface roughness (S_a) as measured using the technique outlined in Topography & wear measurements was 0.23 µm.

Previous studies regarding their application within EV transmission systems have involved the comparison of various base oils, in the absence of commercially available additive packages.²⁹ Therefore, the three lubricants used in this study were a group IV poly- α -olefin (PAO 4) synthetic base oil and two commercially available transmission fluids. One transmission fluid is currently implemented within ICE vehicle dual-clutch transmissions, whereas the second fluid is a factory-fill and service-fill for EV transmission systems. PAO 4 is often used as the base oil for both ICE and EV fluids, and therefore its involvement in this study allows for the influence of application-specific additive packages to be investigated. This category of synthetic base oil typically demonstrates better thermal and dielectric performance than mineral oils in critical applications.³⁰ The inclusion of the ICE fluid in this study allows for the direct comparison of the two commercial fluids and their respective behaviours within an EV representative environment. The viscosity of the lubricants was also measured at 40°C and 100°C using a rheometer. These viscosities are provided by the manufacturer (Lubrizol, UK) and are summarised in Table 2, alongside measured values for conductivity (σ) and dielectric constant (ϵ_r).

Applied electrical potential

Previous studies have investigated the influence of an applied direct current (DC) across unidirectional sliding contacts.³² Under DC conditions ($f = 0$), the resulting current trace ($I(t)$) is solely proportional to the applied DC potential ($V(t) = V_{DC}$) and the conductance (G) of the contact. However, this case does not represent the application of high-frequency AC potentials encountered within

Table 2. Viscosity and dielectric properties of the oils tested.

Property	PAO base oil (Group IV)	ICE transmission fluid	EV transmission fluid
Conductivity (σ) at 90°C (S cm ⁻¹)	–	3.07×10^{-9}	6.71×10^{-10}
Dielectric constant (ϵ_r) at 90°C & 50 Hz	~ 2.09 ³¹	2.41	2.11
Viscosity (η) at 40°C, (cSt)	16.8	31.5	36.8
Viscosity (η) at 100°C, (cSt)	3.8	6.7	7.2

EV applications.⁵ When considering the influence of these potentials, the capacitive nature of dielectric media cannot be overlooked. Therefore, the implications of AC potentials must be considered. Previous research conducted by Yu et al.³³ have also implemented electrical impedance spectroscopy (EIS) using low-amplitude (10 mV) AC potentials at a wide range of frequencies to determine the resistive and capacitive elements of a unidirectional rolling contact. Whilst such tests were designed to be non-destructive – owing to the low observed current magnitudes – a similar analysis procedure may be implemented using potentials that are more representative of an EV environment. Their findings indicate that capacitive effects reduce the overall electrical impedance of such contacts by several orders of magnitude at frequencies above 10⁴ Hz. Whilst such frequencies are beyond the current scope of this study, the effects of low-frequency AC electrification on the tribological processes that occur within these contacts also remains a key obstacle in optimising the tribology and longevity of EV drivetrains.

In this study, a variable alternating current (VariAC) auto-transformer was used to apply an AC potential ($V(t)$) at a frequency (f) of 50 Hz to the sliding ball-on-disc contact, which is immersed in the lubricant variants. This VariAC output was directly attached to the upper ball sample, which was electrically isolated from the load cell and surrounding apparatus using an insulating suspension arrangement. The lower sample was directly fastened to the conductive lubricant bath, which in turn was fastened to an underlying polished brass rotor. A carbon motor brush was placed in contact with the brass rotor and connected to the opposing end of the VariAC output. The lubricant bath was electrically isolated from the rotary drive unit using an insulating polyether ether ketone (PEEK) drive mount – and was also isolated from the surrounding heating unit using a 1 mm air gap.

Magdun et al.¹³ found that a 1.5 kW induction motor can produce stray currents ranging from 0.2–1.4 A. Tischmacher et al.³⁴ also concluded that electric vehicle electric discharges often experience a peak current of around a few amperes. Therefore, an I_{RMS} value of 2 A was selected to imitate a harsher testing environment condition than typically observed. A separate control system was implemented to adjust the RMS magnitude of the applied alternating potential (V_{RMS}) in order to maintain a consistent RMS current magnitude (I_{RMS}) across the contact for the duration of each test.

Topography & wear measurements

An NPFLEX (Bruker, USA) white light interferometer and the Vision64 software package was used to produce 3D

surface heightmaps of sample surfaces prior to testing via a vertical scanning interferometry (VSI) technique. Vision64 was used to measure wear volume loss from ball samples after each test. In addition to measuring cross-sectional volume loss at 4 points around the circumference of each disc sample. The wear measured wear volume on each disc sample was found to be negligible in comparison to their inherent surface roughness, therefore the volume loss measured from each ball sample was taken as an absolute value for each test repeat. The ball samples were also examined and measured using an optical microscope (Leica DM6000M) and a scanning electron microscope (Hitachi TM4000 Plus benchtop SEM).

An in-house MATLAB program was used to produce gradient magnitude and directionality maps for each surface. These images were created by using the difference in height between each individual datum and its adjacent datums across the surface to determine the steepness and direction of the surface at each individual point of the image.

Chemical analyses

Inductively coupled plasma (ICP) spectroscopy carried out by Lubrizol; UK was used to identify the key additive components in the two commercial transmission fluids.

A Thermo Fisher Scientific Nicolet iS10 spectrometer was also used to perform Fourier transform infra-red (FTIR) spectroscopy in the wavelength range between 400–4000 cm⁻¹ on the lubricants prior to and post-testing. Energy Dispersive Spectroscopy (EDX), using a Bruker Quantax 75 EDX system was also implemented in conjunction with the Hitachi TM4000 Plus SEM measurements in order to characterise the surface elemental composition of the ball and disc samples after testing.

Results & discussion

Lubricant properties

Table 2 summarises the mechanical and electrical properties of the lubricants in this study. The EV transmission fluid exhibited an increased viscosity when compared to the ICE transmission fluid at both 40 and 9° C. PAO 4 exhibited the lowest viscosity. The EV transmission fluid exhibits a lower conductivity and dielectric constant when compared to its ICE counterpart. This indicates that the EV transmission fluid has a lower permittivity to both DC and AC electrification. The PAO 4 base oil understandably exhibited the lowest dielectric constant, owing to the distinct lack of polar

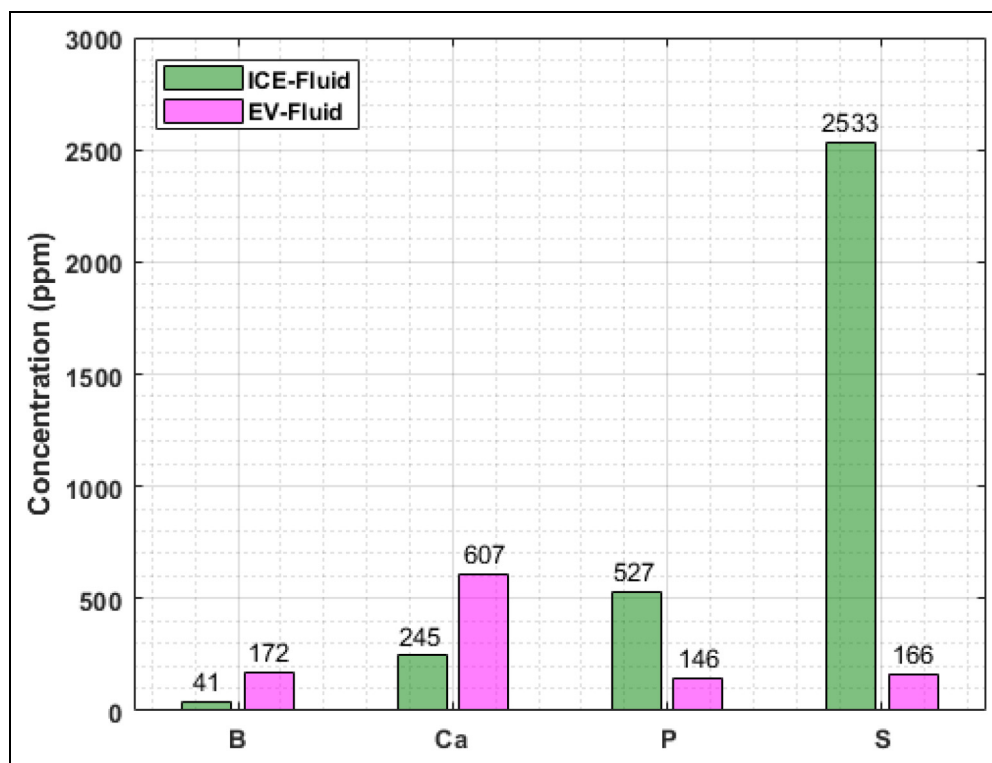


Figure 2. Elemental composition of transmission lubricants as measured using inductively coupled plasma spectroscopy (ICP).

additives within its composition. The elemental compositions of the pre-test oils given by ICP analysis are shown in Figure 2.

Friction measurements

Figure 3(a) shows the average coefficient of friction trends over two hours for the three lubricant variants at two different levels of electrification, whilst Figure 3(b) highlights the time-averaged coefficient of friction (CoF) for the final thirty minutes of each test. Overall, the PAO 4 lubricants had the highest friction response whereas the EV fluid had the lowest. The Figures also show that with the formulated oils a reduction in friction is observed under electrified conditions. With majority of the tests (electrified and unelectrified) the transient data shows an initial high CoF before steady state is reached, most likely due to the 'running-in' of the samples. A key trend observed from the tests was the increase of friction from 0.13 to 0.145 with PAO 4 with the application of a potential, but with the formulated oils a decrease was observed. The PAO 4 tests also exhibited a significantly higher degree of variance in friction between tests. From all test conditions the lowest friction coefficients were the unelectrified PAO 4 and the electrified EV transmission fluid, whereas the electrified PAO 4 yielded the highest overall friction coefficient.

Previous studies have highlighted that the observed reduction in coefficient of friction under electrified conditions could be a result of several mechanisms. The electrochemically driven formation of passive oxide layers³⁵ and additive films, in addition to the charge-promoted

adsorption of surface ions have previously been shown to influence friction performance.²² The application of an electric potential to a lubricant can also cause its degradation, in addition to degradation to any constituent additive packages.²²

Zhu et al.³⁶ found that applying an electric potential to sliding iron-on-iron contacts led to a decrease in friction behaviour but a significant increase in wear. It was believed this was due to the conversion of iron oxides (Fe_3O_4) to iron oxyhydroxides (FeOOH). Brandon et al.³⁷ proposed that the adsorption of surfactants to form a protective, friction-reducing film could be increased through the application of an electric potential. Zhu et al.³⁶ found that the presence of redox reactions and subsequent chemical modification of a metallic surface can influence the level of interaction of lubricant surfactants with the surface. Since the PAO 4 base oil contained no additives, the likelihood of low-friction tribofilm formation under electrified conditions is significantly lower. Therefore, the dominant electrochemical mechanism under electrified conditions will be the degradation of the lubricant itself, leading to the higher friction behaviour observed.

When comparing the friction behaviour of the two transmission fluids under unelectrified conditions, the ICE transmission fluid demonstrated higher friction behaviour for majority of the test duration. This elevated friction coefficient does eventually lower to a value below that of the EV equivalent after 6600 s of testing. This eventual reduction of friction may be also due to the difference in the formation rates and coverage of an effective tribofilm with the ICE fluid, in-comparison to

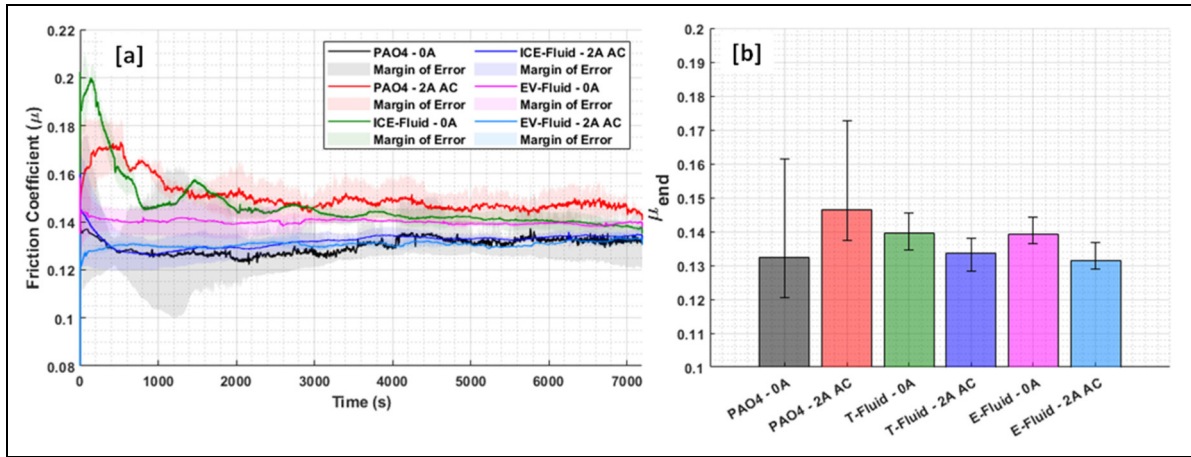


Figure 3. Average friction coefficient versus time results over (a) 2 h and (b) the last 30 min of the experiments for the three lubricant variants with unelectrified and electrified conditions.

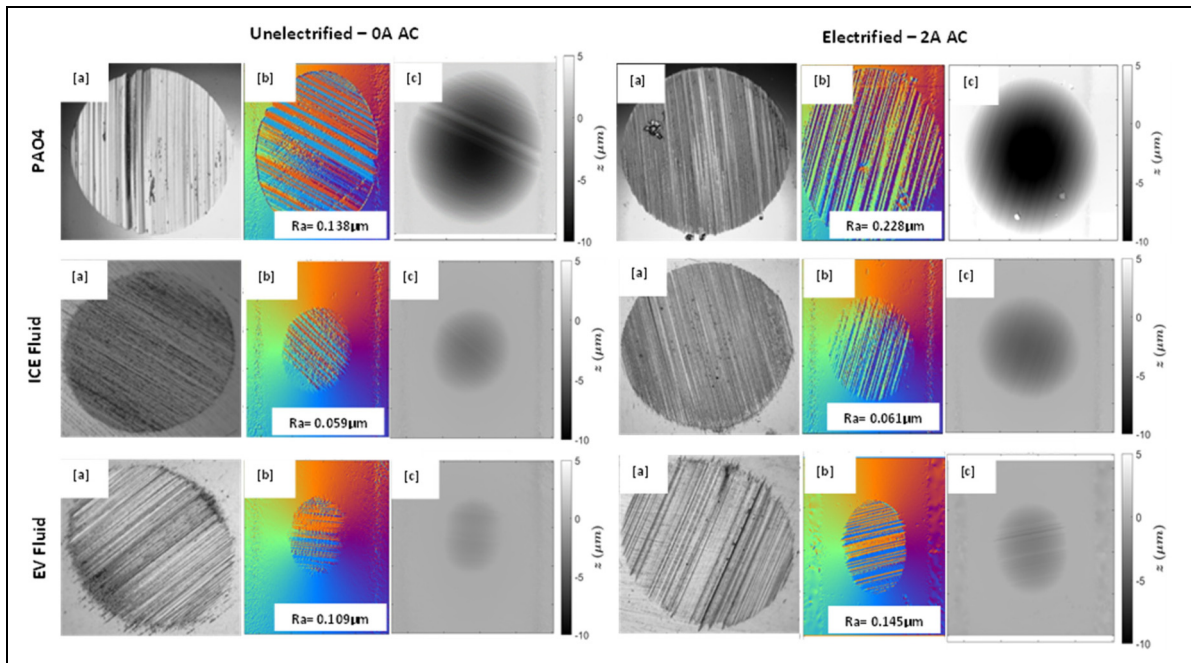


Figure 4. Optical image, (b) gradient directionality map, and (c) height map of the ball wear scar regions for the three lubricant variants under unelectrified and electrified conditions.

the EV alternative. Overall, the average friction coefficient of the EV fluid for the last 30 min of testing was lower than the ICE transmission fluid.

However, with electrified conditions the EV fluid maintained a constant lower friction trend compared to the ICE transmission fluid. Initially lower friction behaviour was observed with the ICE fluid, until this deteriorated and a higher friction trend was exhibited for the remainder of the test. This deterioration in friction trend with the ICE transmission fluid was not observed under unelectrified conditions, indicating the application of an AC potential could be the cause of fluid property deterioration. The higher friction behaviour initially observed with the EV fluid compared to the ICE fluid alternative may be also a

result of its lower fluid viscosity, leading to a lubrication regime closer to boundary conditions as opposed to a mixed regime.³⁸ The low dielectric constant of the EV transmission fluid aids in lowering its reactance to alternating electric fields and resulting polarizability preventing its deterioration over time with the application of a potential. The presence of boron compounds within the EV transmission fluid also helps to promote thermal and oxidation stability.⁵ Boron additives can react with iron oxide surfaces and lead to the formation of a hard, protective borate-iron glassy layer.³⁹ Tang et al.⁴⁰ found that a balanced detergent/dispersant additive system – post-treated with boron and phosphorus compounds could provide a low electrical conductivity in combination with improved friction and

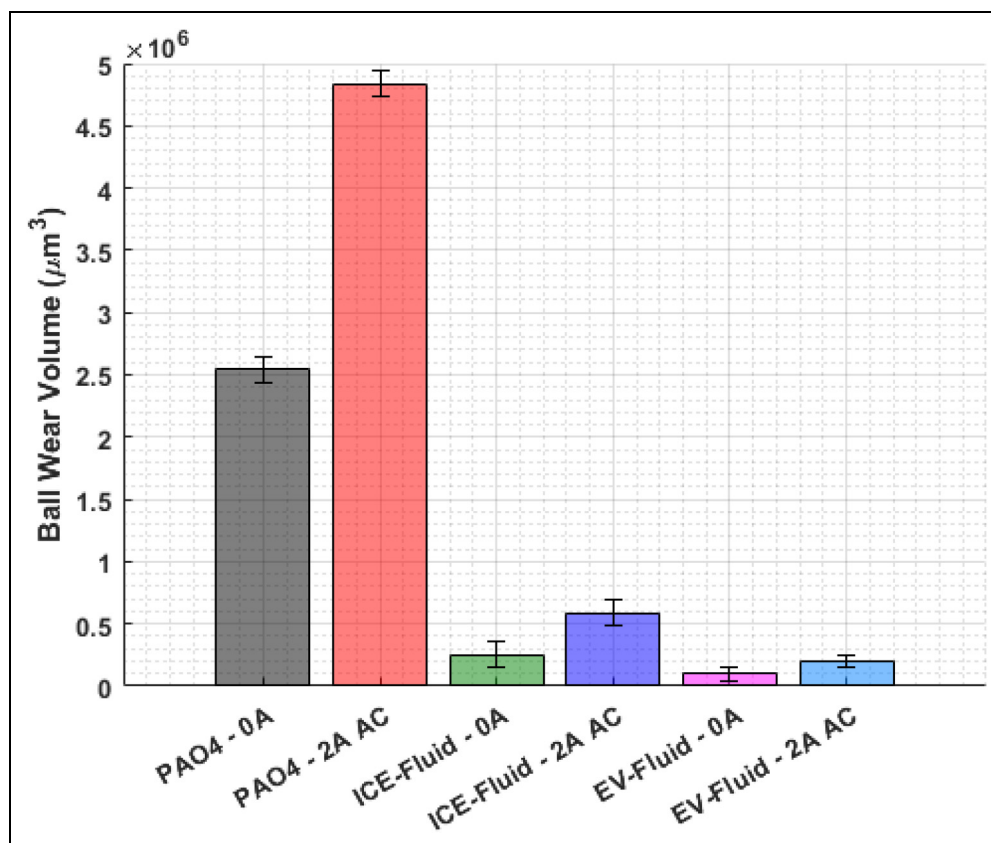


Figure 5. Volume loss of the ball samples for the three lubricant variants with unelectrified and electrified conditions

anti-wear properties. Cao-Romero-Gallegos et al.⁴¹ concluded that higher temperatures are to be expected at the local asperities within electrified contacts. This increased ‘flash’ temperature could lead to chemical degradation of the lubricant, or influence tribofilm formation rate.

Topography & wear measurements

Figure 4(a) shows example optical images of the ball wear scars for each lubricant under both electrification conditions. The images highlight the surface topography features post-testing allowing for any changes due to electrification conditions or lubricant variation to be highlighted. Figure 4(b) shows colourmaps that represent the directionality of the gradient at each point on the uncorrected heightmap. The colourmaps help to distinguish and identify key surface features such as abrasive wear. Strong evidence of abrasive scoring is enhanced and depicted as the contrasting unidirectional patterns seen within each wear area. It is also evident that the diameter of the wear area on each ball is contracted in the direction of sliding, indicative of the tangential nature of the forces and resulting deformations encountered within the contact. The colourmaps (Figure 4(b)) also highlight the surface roughness (R_a) values post-experiment, with PAO 4 and ICE fluid lubricated surfaces having the highest and lowest roughness’s respectively. The analysis also showed an increase in surface roughness under electrified conditions with all

lubricant variants, potentially due to the increased abrasive wearing occurring under these conditions. Figure 4(c) shows example heightmaps of the ball surfaces, corrected to account for their respective spherical curvatures. The wear volume of each ball sample was taken from these heightmaps, where darker regions indicated higher wear depths. It is possible to see PAO 4 fluid generated the highest depths of wear compared to the formulated lubricants, where the EV fluid had the least wear. It is also possible to see darker and hence deeper regions of wear under electrified conditions with all three lubricant variants. From the coloured maps and the height maps it is easier to observe higher amounts of abrasive wear and increased wear respectively, in the wear scars of the ball samples under electrified conditions for all three lubricant variants. This is believed to be caused by abrasive debris detached from an oxide formed due to the electrification formation mechanics as discussed in Friction measurements.³⁵

The average wear volumes from ball samples under each test condition are depicted in Figure 5. Upon examination it becomes clear that the pure PAO 4 base oil exhibits significantly elevated rates of material wear when compared to contacts lubricated by the two formulated transmission fluids. This is expected and a direct result of the PAO 4 base oil containing no additional property-modifying or wear-preventing additives in its composition. Additionally, the additive packages contained within the two commercial transmission fluids are

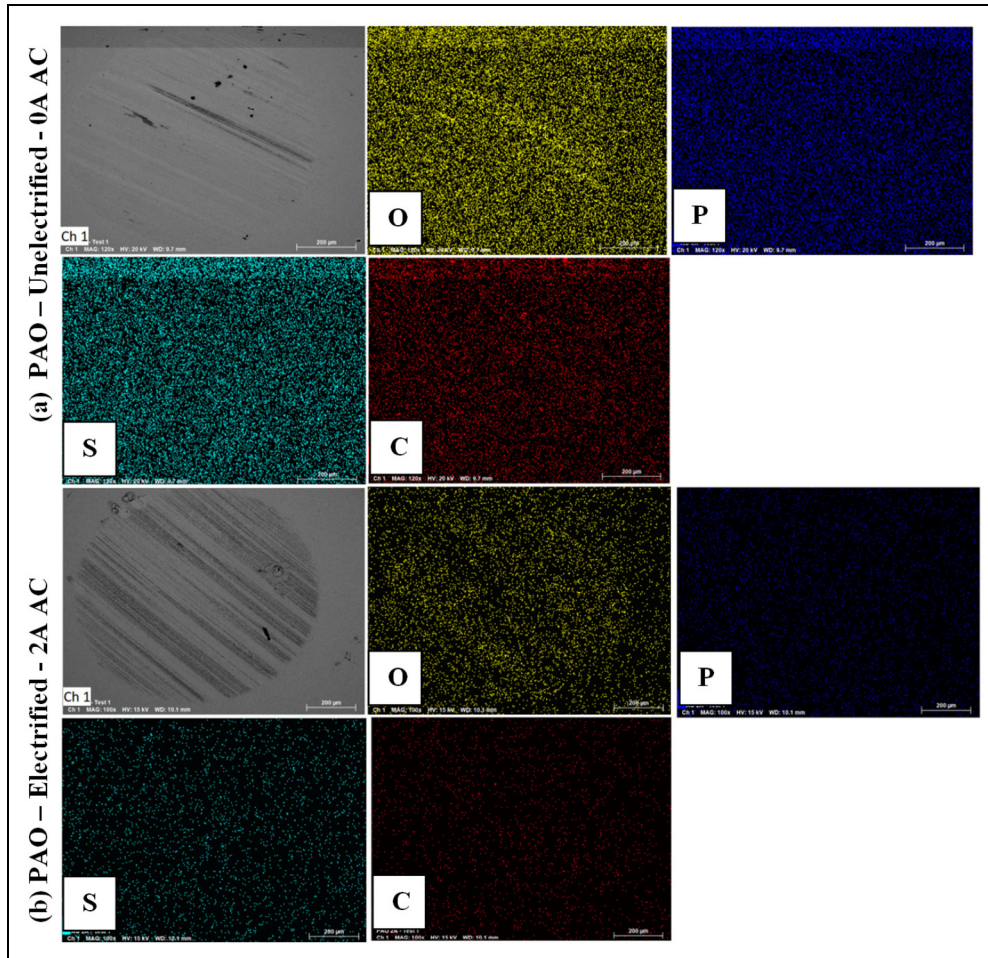


Figure 6. SEM and EDX images of ball wear scar with the PAO 4 lubricant when (a) unelectrified and (b) electrified. Elements mapped are O, P, S & C.

formulated to reduce friction and wear through the formation of a protective tribofilm formation under certain conditions.⁴² The EV transmission fluid is also shown to exhibit less material wear than the ICE equivalent under both AC-electrified and unelectrified conditions. This may be due to the higher viscosity properties of the EV fluid and the presence of boron compounds, which have been shown to improve the extreme-pressure and anti-wear properties of gear oils.⁵ ICP analysis also showed that the EV fluid had a less active sulphur content when compared to the traditional ICE transmission fluid. The EV transmission fluid has a significantly lower concentration of active sulphur content to avoid the risk of producing copper sulphides or sulphate (CuSO_4) via corrosive mechanisms within EV drivetrains.^{43,44}

The most prominent observed trend is that AC-electrification is shown to increase the wear rate for contacts lubricated by all three fluids. This increase in wear resulting from electrification maybe a result of oxidation at the contact interface, as seen by other studies which also utilised AISI 52100 bearing steel.³² Farfan-Cabrera³² found that the application of a current significantly increased oxidation and the formation of hematite ($\alpha\text{-Fe}_2\text{O}_3$) oxides at the wearing interface. These oxides

can become detached during sliding and subsequently form debris to accelerate third-body abrasive wear.³⁵ Overall, the EV transmission fluid gave lower wear when electrified compared to the transmission fluid. This is likely a combination of the higher viscosity, lower conductivity, and lower dielectric constant of the EV transmission fluid.

Chemical analysis – EDX

EDX has been utilised to understand and identify the chemical formations occurring at the contact during testing with the three lubricant variants and the impact of electrification on these formations. Figure 6(a) and (b) depict EDX spatial maps (O, P, S & C) of the worn ball samples when using unelectrified and electrified conditions respectively, with the PAO 4 lubricant. The PAO 4 lubricant contained no additive package, therefore no phosphorus (P), sulphur (S), boron (B) or calcium (Ca) were detected in the wear area. With the absence of additive packages, the high wear observed in Figure 5 with the PAO 4 is expected. Traces of oxidation are observed in the wear area under both conditions, with the electrified samples showing an

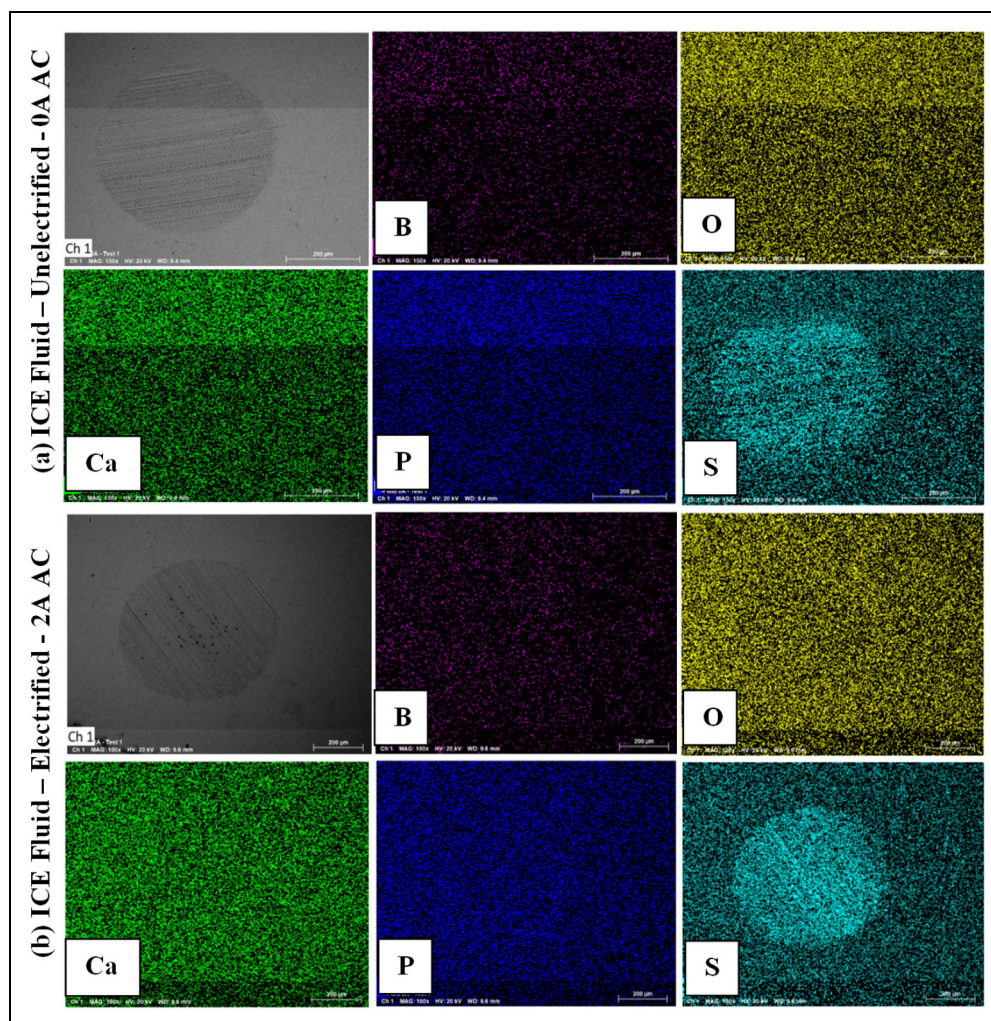


Figure 7. SEM and EDX images of ball wear scar with the ICE transmission lubricant when (a) unelectrified and (b) electrified. Elements mapped are B, O, Ca, P & S.

elevated concentration of surface oxides. This finding supports the theory that AC-electrification encourages surface oxidation. These oxidation sites are consistent with the darker patches on the surfaces as observed in both the SEM and optical images.

Figure 7(a) and (b) show the EDX maps (B, O, Ca, P & S) of the worn ball samples when using unelectrified and electrified conditions respectively, with the ICE transmission fluid. As shown in Figure 7, the ICE transmission fluid contains high amounts of sulphur, as an extreme pressure additive, which was also strongly observed in the wear scars of both electrified and unelectrified samples. The high sulphur content in the transmission fluid which correlates to the EDX map results of the worn area. Sulphur-containing compounds help to mitigate the process of scuffing under severe operating conditions.⁴⁵ The formation of a sulphur containing protective layer would impact friction and wear behaviour and would account for the lower wear volume loss (Figure 5) in comparison to just using PAO 4. The EDX maps of the electrified surface (Figure 7(b)) showed an increased surface coverage by sulphur, supporting Zhu et al.'s³⁶ theory that surfactants in the lubricant can

interact with the oxidised or reduced surface due to electrification and encourage the formation of a thicker or wider covering tribofilm. Electrification may also have also caused an increase in surface roughness, which in-turn may have increased mechanical interactions between two surfaces encouraging an increased activation of the lubricant additives hence a thicker tribofilm was observed under electrified conditions. The higher presence of sulphur in the tribofilm due to electrification conditions could also encourage the formation of FeS. The increased presence of FeS would impact friction behaviour and could account for the lower friction observed compared to unelectrified conditions. The presence of a coherent thicker FeS tribofilm would help to reduce friction behaviour in-comparison to a patchier thinner film. Farfan-Cabrera³² found that the application of a potential could contribute to the fast and easy formation of a combined oxide-rich tribofilm from anti-friction and wear additives. It is believed more effective boundary films are formed through the activation of additives by an increase in flash temperatures at real contact spots where the electric current is mostly discharged. The increase in wear with

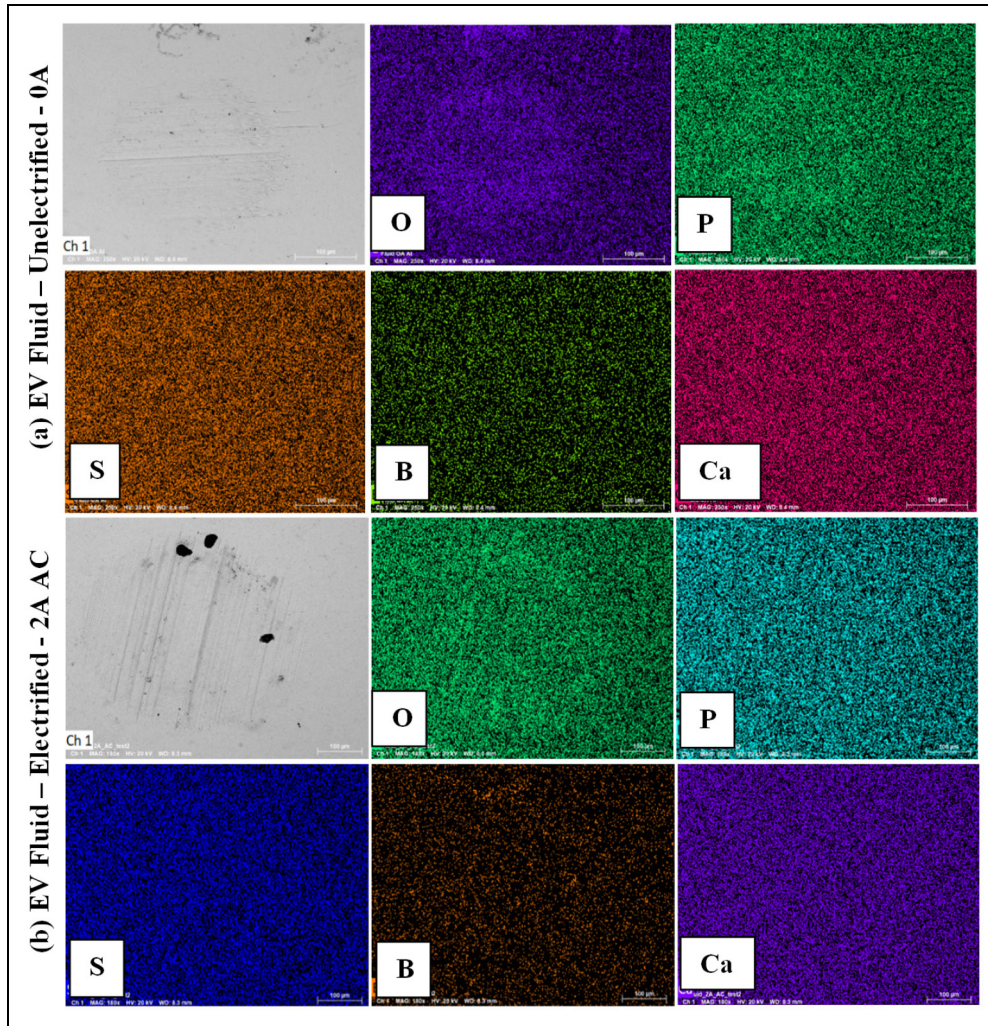


Figure 8. SEM and EDX images of ball wear scar with the EV transmission lubricant when (a) unelectrified and (b) electrified. Elements mapped are O, P, S, B & Ca.

electrification could also lead to an increase in contact area and the presence of a less severe boundary regime and reduce friction. No other chemical elements are identified in the wear scars, the heavy coverage of the surface by sulphur may have made it difficult to identify the oxidation of the surface.

Figure 8(a) and (b) show the EDX maps (O, P, S, B & Ca) of the worn ball samples when using unelectrified and electrified conditions respectively, with the EV fluid. As highlighted in Figure 2, the EV transmission fluid contains B, Ca, P & S and in Figure 8(a) with the unelectrified conditions traces of phosphorus can be seen in the wear scar. The formation of an anti-wear protective layer would impact friction and wear behaviour and could account for the lowest wear loss observed from all the fluid variants (Figure 5). Phosphorus additives are effectively used for anti-wear protection.⁴⁶ Traces of phosphorus is also seen in Figure 8(b) when using the electrified conditions supporting the low wear behaviour also observed in this testing condition. With both testing conditions with the EV fluid (Figure 8(a) and (b)) the presence of oxides

were present in the wear scar, which may play a role in the formation mechanics of the tribofilm. The presence of surfactants in the lubricant combined with the oxidation or reduction of the metal surfaces can change the formation mechanics of those surfactants with such surfaces.²² Other studies have shown that the reduction of the coefficient of friction was promoted by the application of a potential was due to the fast and easy formation of an oxide tribofilm.^{22,32}

Chemical analysis – FTIR

FT-IR is applied to study the functional group variations with the different lubricating oils and testing conditions used in this paper. Three variant conditions of each lubricant were analysed – neat (unused), unelectrified and electrified. Several functional groups were common to the different lubricant types (a – PAO, b – ICE Fluid & c – EV Fluid) as seen in Figure 9. The bands at ~ 2957 , ~ 2925 , and $\sim 2854 \text{ cm}^{-1}$ were attributed to aliphatic –

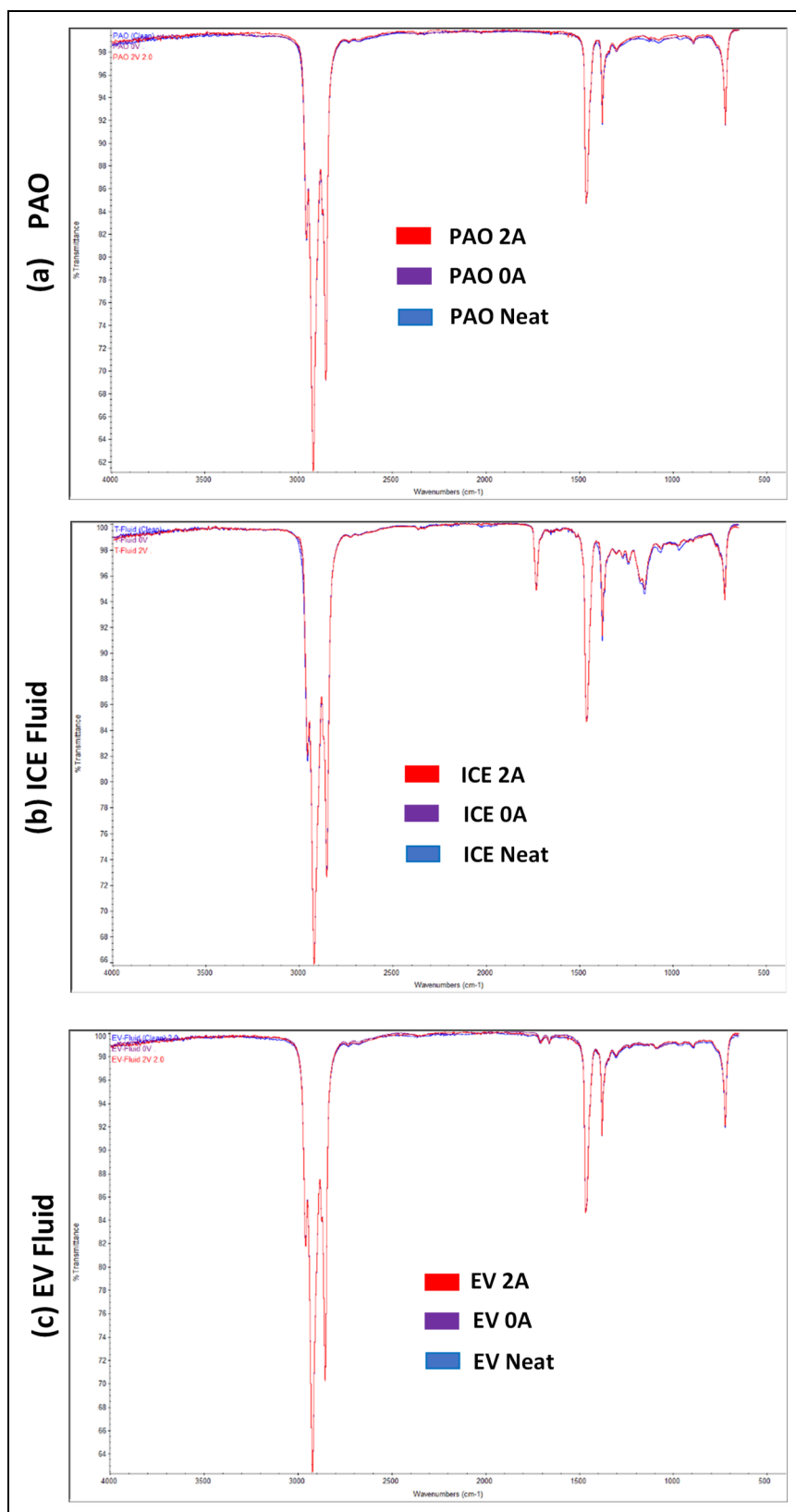


Figure 9. Fourier-Transform infrared (IR) spectroscopy spectra obtained for (a) PAO 4, (b) ICE fluid and (c) EV fluid when unused, unelectrified and electrified.

CH_3 and $-\text{CH}_2$ symmetric stretching and asymmetric stretching modes of the ethylene groups from the alkyl chains.⁴⁷ The peak observed at $\sim 1741\text{cm}^{-1}$ could be attributed to $\text{C}=\text{O}$ stretching vibration in saturated fatty acid

esters. The peak at $\sim 1465\text{cm}^{-1}$ corresponds to CH_2 vibrations and peak $\sim 1378\text{cm}^{-1}$ was assigned to the C–H deformation vibration of $-\text{CH}(\text{CH}_3)_2$ aliphatic chains.⁴⁸ The peaks seen at ~ 3645 and $\sim 686\text{cm}^{-1}$ can be attributed

to O–H stretching vibrations and O–H curling vibrations, respectively.^{8,49} The peak at $\sim 1150\text{ cm}^{-1}$ could be attributed to sulfonyl stretch from the sulphur which was present in the two commercial transmission fluid.⁵⁰ In Figure 9(b), with the ICE transmission fluid sharp and strong sulphur bands are seen with all testing variants and corresponds with the strong detection of sulphur in the EDX maps as seen in Figure 8. The sulphur band is also seen with the EV transmission fluid (Figure 9(c)) which also contained sulphur. From Figure 9(a)–(c) it is possible to see with all lubricant variants and the different testing conditions, there were no change to the chemical structure of the lubricant. By comparing the FTIR curves of the neat oil and the oil from the unelectrified tests which were carried out at 80°C , no signs of changes to the graphs can be observed, indicating thermal degradation was not occurring and similar trends are observed when the lubricant was electrified. These trends were similar to that reported by Tormos et al.⁵¹ with base oil variants used for e-fluids and Rodriguez et al.⁸ with varying conditions of transmission fluids for EV's. However, the changes due to thermal degradation or electrification may not have been detected due to the short duration of the test which may not have caused the lubricant to degrade to a level which may have been detected with FTIR.

Conclusions

The aim of this study was to utilise a ball-on-disc experimental set-up to understand the effects of AC electrification (2 A) on the friction and wear behaviour of gear steel material when using three different lubricants (PAO 4 base oil, ICE transmission oil and EV transmission oil). The key conclusions drawn from the work are:

- With the commercial transmission fluids, with electrification the COF of the two fluids decreased and this is believed due to the formation of a passivating oxide layer. This could be due to the adsorption of ions from the lubricant additives or oil molecules and redox reactions leading to an increase in metal oxide formation.
- Electrification may roughen the surface which would increase mechanical interactions between surfaces encouraging an increased activation of the lubricant additives.
- The presence of surfactants in the lubricant can interact with the oxidised or reduced metallic surface and further influence tribological behaviour.
- The electrified surfaces had higher wear loss with the two commercial transmission fluids. This is believed due to the wear of oxidised layer forming on the surface due to electrification. The electrified surfaces had higher signs of abrasive wear due to these oxidised wear debris interacting in the contact zone. Overall, the EV fluid showed the lowest wear compared to the other fluid variants used in this study.
- FTIR indicated that electrification or heating to 80°C seemed to have no real effect on causing chemical changes with all the lubricants used in this study.

- A novel modified set-up of a ball-on-disc tribometer was shown to be effective in performing electrified sliding tests. These tests can be used for fast and effective screening of lubricants and materials that would be used in electrified environments from gears in electric vehicles to electricity powered drivelines.

Acknowledgments

We would like to thank Lubrizol Corporation for their donation of a requested e-fluid and dual-clutch transmission fluid to enable our independent research. This work was supported by the Engineering and Physical Sciences Research Council [EP/X023389/1].

Credit statements

Thawhid Khan: Conceptualisation, Methodology, Investigation, Writing – Original Draft. Joshua Armitage: Conceptualisation, Investigation, Methodology, Writing – Original Draft. Michael Bryant: Conceptualisation, Resources, Supervision, Writing – Original Draft.

Data availability

Data will be made available on request.

Declaration of conflicting interests

The authors declared no potential conflicts of interest with respect to the research, authorship, and/or publication of this article.


Funding

The authors disclosed receipt of the following financial support for the research, authorship, and/or publication of this article: This work was supported by the Engineering and Physical Sciences Research Council (grant number EP/X023389/1).

Statement of originality

The work presented in this manuscript is, to the best of my knowledge and belief, original, except as acknowledged in the text. The present work has not been published elsewhere and is not being submitted to any other journals.

ORCID iD

Thawhid Khan  <https://orcid.org/0000-0001-9621-9928>

References

1. Roge OCVGTA. *CO2 Emissions in 2022*. 2022, p.19.
2. Shadidi B, Najafi G and Yusaf T. A review of hydrogen as a fuel in internal combustion engines. *Energies* 2021; 14: 6209.
3. Tornatore C, Marchitto L, Sabia P, et al. Ammonia as green fuel in internal combustion engines: state-of-the-art and future perspectives. *Front Mech Eng* 2022; 8: 72.

4. Cai W, Wu X, Zhou M, et al. Review and development of electric motor systems and electric powertrains for new energy vehicles. *Automotive Innov* 2021; 4: 3–22.
5. Farfan-Cabrera LI. Tribology of electric vehicles: a review of critical components, current state and future improvement trends. *Tribol Int* 2019; 138: 473–486.
6. Holmberg K and Erdemir A. The impact of tribology on energy use and CO₂ emission globally and in combustion engine and electric cars. *Tribol Int* 2019; 135: 389–396.
7. Previati G, Mastinu G and Gobbi M. Thermal management of electrified vehicles—A review. *Energies* 2022; 15: 1326.
8. Rodríguez E, Rivera N, Fernández-González A, et al. Electrical compatibility of transmission fluids in electric vehicles. *Tribol Int* 2022; 171: 107544.
9. McCoy B. *Next generation driveline lubricants for electrified vehicles*. 2021, https://www.stle.org/files/TLTArchives/2021/03_March/Webinar.aspx.
10. Gahagan MP. *Lubricant technology for hybrid electric automatic transmissions*. Berlin, Germany: SAE Technical Paper, 2017.
11. Vijaya Sambhavi Y and Ramachandran V. A technical review of modern traction inverter systems used in electric vehicle application. *Energy Rep* 2023; 10: 3882–3907.
12. He F, Xie G and Luo J. Electrical bearing failures in electric vehicles. *Friction* 2020; 8: 4–28.
13. Magdun O, Gemeinder Y and Binder A. Investigation of influence of bearing load and bearing temperature on EDM bearing currents. In: 2010 IEEE energy conversion congress and exposition, 2010.
14. Jaritz M, Jaeger C, Bucher M, et al. An improved model for circulating bearing currents in inverter-fed AC machines. In: 2019 IEEE international conference on industrial technology (ICIT), 2019.
15. Punga F and Hess W. Eine Erscheinung an Wechsel- und Drehstromgeneratoren. *Elektrotechnik und Maschinenbau* 1907; 25: 615–618.
16. Fleischmann L. Ströme in Lagern und Wellen. *Elektr Kraftbetriebe Bahnen* 1909; 7: 352–353.
17. Alger PL and Samson HW. Shaft currents in electric machines. *J Am Inst Electr Eng* 1923; 42: 1325–1334.
18. Esmacili K, Wang L, Harvey TJ, et al. Electrical discharges in oil-lubricated rolling contacts and their detection using electrostatic sensing technique. *Sensors* 2022; 22: 392.
19. Cao-Romero-Gallegos JA, Reyes-Avenidaño J, Soriano J, et al. *A pin-on-disc study on the electrified sliding wear of EVs powertrain gears*. Warrendale, PA, USA: SAE International, 2022.
20. Chapter 6 measurement of fluid film thickness and detection of film failure. In: Dorinson A and Ludema KC (eds) *Tribology series*. Amsterdam, Netherlands: Elsevier, 1985, pp.109–133. <https://www.sciencedirect.com/science/article/abs/pii/S0167892208708459>
21. Anno J. AC Breakdown voltage for a thin dielectric fluid film. *J Appl Phys* 1968; 39: 4326–4328.
22. Spikes HA. Triboelectrochemistry: influence of applied electrical potentials on friction and wear of lubricated contacts. *Tribol Lett* 2020; 68: 90.
23. Zhu Y, Ogano S, Kelsall G, et al. The study of lubricant additive reactions using non-aqueous electrochemistry. *Tribol Trans* 2000; 43: 175–186.
24. Chang Q, Meng Y and Wen S. Influence of interfacial potential on the tribological behavior of brass/silicon dioxide rubbing couple. *Appl Surf Sci* 2002; 202: 120–125.
25. Xu X and Spikes H. Study of zinc dialkyldithiophosphate in di-ethylhexyl sebacate using electrochemical techniques. *Tribol Lett* 2007; 25: 141–148.
26. Kai N, Chenfei S, Zhihao L, et al. Electric damage of bearing under AC shaft voltage at different rotation speeds. *Tribol Int* 2023; 177: 108008.
27. Bleger A, Leighton M and Morris N. Automotive e-motor bearing electrical discharge phenomena: an experimental and numerical investigation. *Tribol Int* 2024; 191: 109140.
28. Li X and Olofsson U. FZG Gear efficiency and pin-on-disc frictional study of sintered and wrought steel gear materials. *Tribol Lett* 2015; 60: 1–10.
29. Guo L, Mol H, Nijdam T, et al. Study on the electric discharge behaviour of a single contact in EV motor bearings. *Tribol Int* 2023; 187: 108743.
30. Mobil E. *Driveline fluids for electric vehicles*. [cited 2024], <https://www.exxonmobilchemical.com/en/products/synthetic-base-stocks/electric-vehicle-fluids/electric-vehicles-driveline-fluids>.
31. Mobil E. *SpectraSyn Plus™ Polyalphaolefins (PAO)*. 2006, p.2.
32. Farfan-Cabrera LI, Erdemir A, Cao-Romero-Gallegos JA, et al. Electrification effects on dry and lubricated sliding wear of bearing steel interfaces. *Wear* 2023; 516: 204592.
33. Yu M, Zhang J, Joedicke A, et al. Using electrical impedance spectroscopy to identify equivalent circuit models of lubricated contacts with complex geometry: in-situ application to mini traction machine. *Tribol Int* 2024; 192: 109286.
34. Tischmacher H, Gattermann S, Kriese M, et al. Bearing wear caused by converter-induced bearing currents. In: IECON 2010 – 36th annual conference on IEEE industrial electronics society, 2010.
35. Pearson BR, Brook PA and Waterhouse RB. Influence of electrochemical potential on the wear of metals, particularly nickel. *Tribol Int* 1988; 21: 191–197.
36. Zhu YY, Kelsall GH and Spikes HA. The influence of electrochemical potentials on the friction and wear of iron and iron oxides in aqueous systems. *Tribol Trans* 1994; 37: 811–819.
37. Brandon N, Bonanos N, Fogarty P, et al. The effect of interfacial potential on friction in a model aqueous lubricant. *J Electrochem Soc* 1992; 139: 3489.
38. Skaltsas D, Rossopoulos GN and Papadopoulos CI. A comparative study of the Reynolds equation solution for slider and journal bearings with stochastic roughness on the stator and the rotor. *Tribol Int* 2022; 167: 107410.
39. Sr DB. Using conventional molybdenum and boron lubricant additives in electric vehicles. In: *Lube: the European lubricants industry magazine*, 2024, p.8.
40. Tang TH-Z, Devlin M, Mathur N, et al. Lubricants for (hybrid) electric transmissions. *SAE Int J Fuels Lubr* 2013; 6: 289–294.
41. Cao-Romero-Gallegos JA, Farfan-Cabrera LI, Erdemir A, et al. Lubricated sliding wear of gear material under electrification—A new approach to understanding of the influence of shaft currents in the wear of EV transmissions. *Wear* 2023; 523: 204782.
42. Konicek AR, Jacobs PW, Webster MN, et al. Role of tribofilms in wear protection. *Tribol Int* 2016; 94: 14–19.

43. Rensselaar J. Driveline fluids for electric vehicles. *Tribol Lubr Technol* 2021; 77: 42–47.
44. *Lubrizol introduces new sulfur-free driveline lubricant technology for EV transmissions and e-axes*. [cited 2024], <https://chargedevs.com/whitepapers/lubrizol-introduces-new-sulfur-free-driveline-lubricant-technology-for-electric-vehicle-ev-transmissions-and-e-axes/>.
45. Khorramian B, Iyer G, Kodali S, et al. Review of antiwear additives for crankcase oils. *Wear* 1993; 169: 87–95.
46. Spikes H. Low-and zero-sulphated ash, phosphorus and sulphur anti-wear additives for engine oils. *Lubr Sc* 2008; 20: 103–136.
47. Chimeno-Trinchet C, Pacheco M, Fernández-González A, et al. New metal-free nanolubricants based on carbon-dots with outstanding antiwear performance. *J IndEng Chem* 2020; 87: 152–161.
48. Socrates G. *Infrared and Raman characteristic group frequencies: tables and charts*. Hoboken, NJ, USA: John Wiley & Sons, 2004.
49. Gan Z, Yao T, Zhang M, et al. Effect of temperature on the composition of a synthetic hydrocarbon aviation lubricating oil. *Materials* 2020; 13: 1606.
50. Rahman NA, Katon MK and Zulkifli NAZ. Analysis of automatic transmission using Fourier transform infrared (ftir) spectroscopy. *e-Acad J* 2019; 7: 58–66.
51. Tormos B, Bermúdez V, Ruiz S, et al. Degradation effects of base oils after thermal and electrical aging for EV thermal fluid applications. *Lubricants* 2023; 11: 241.